

Mechanistic Insight into Catalyst-Controlled Photodegradation of Ru(II) Polypyridyl Complexes

Hadeel Ali Mohammed ^{1*}, Hamid. M. Younis ²


^{1,2} Chemistry Department, Faculty of Science, Sirte University, Sirte-Libya

*Email: hadeel-alsed@su.edu.ly

رؤية ميكانيكية حول التحلل الضوئي المُتَحَكَم فيه بواسطة الحفّاز لمُعَقَّدات الروثينيوم (II) متعددة البيريديل

هديل علي محمد ^{1*} ، حميد محمد يونس ²

^{2,1} قسم الكيمياء، كلية العلوم، جامعة سرت، سرت، ليبيا

Received: 15-01-2026	Accepted: 10-03-2026	Published: 22-03-2026
	Copyright: © 2026 by the authors. This article is an open-access article distributed under the terms and conditions of the Creative Commons Attribution (CC BY) license (https://creativecommons.org/licenses/by/4.0/).	

Abstract

Understanding the mechanisms governing the photodegradation of Ru(II) polypyridyl complexes is essential for the rational design of stable photoactive systems. In this study, mechanistic insight into the catalyst-controlled photodegradation of Ru(II) complexes bearing tbbpy ligands is presented through a comparative investigation of systems with and without a peripheral PtI₂ unit. Photodegradation under visible-light irradiation was monitored by time-dependent UV–Vis spectroscopy and analyzed under pseudo-first-order kinetic conditions in acetonitrile and methanol. Complementary HPLC and ¹H NMR analyses verified that the observed spectral changes arise from irreversible chemical degradation rather than transient photophysical processes. Coordination of the PtI₂ unit significantly modulates the MLCT excited state, leading to a reduced optical gap and prolonged excited-state lifetime, as supported by TD-DFT calculations. Solvent-dependent kinetic behavior further reveals the role of medium coordination in stabilizing the photoexcited state. Collectively, these results provide mechanistic insight into how catalyst coordination governs photodegradation pathways in Ru(II) polypyridyl complexes.

Keywords: (Ruthenium(II) polypyridyl complexes; Photodegradation mechanism; MLCT states; PtI₂ coordination; UV–Vis spectroscopy; Solvent effects) .

الملخص

يُعد فهم الآليات التي تتحكم في التحلل الضوئي لمُعقدات الروثينيوم (II) متعددة البيريدين أمراً أساسياً للتصميم العقلاني لأنظمة ضوئية نشطة مستقرة. في هذه الدراسة، يتم تقديم تحليل ميكانيكي للتحلل الضوئي المُتحكم فيه بواسطة الحفّاز لمُعقدات الروثينيوم (II) الحاملة لربيطات tbbpy، وذلك من خلال دراسة مقارنة للأنظمة بوجود وحدة PtI_2 الطرفية وبدونها. تم تتبع التحلل الضوئي تحت إشعاع الضوء المرئي باستخدام مطيافية الأشعة فوق البنفسجية-المرئية المعتمدة على الزمن، وتحليل النتائج وفق حركية من الدرجة الأولى الزائفة في مذبيبي الأسيتونتريل والميثانول.

أكدت تحاليل HPLC و 1H NMR أن التغيرات الطيفية الملحوظة ناتجة عن تحلل كيميائي غير عكوس، وليس عن عمليات فوتوفيزيائية عابرة. كما أن تنسيق وحدة PtI_2 يؤثر بشكل ملحوظ على حالة انتقال الشحنة معدن-ربيطة (MLCT)، مما يؤدي إلى تقليل الفجوة البصرية وإطالة عمر الحالة المثارة، وهو ما تدعمه حسابات TD-DFT.

كما يُظهر السلوك الحركي المعتمد على نوع المذيب الدور المهم لتناسق الوسط في تثبيت الحالة المثارة ضوئياً. وبشكل عام، تقدم هذه النتائج فهماً ميكانيكياً لكيفية تحكم تنسيق الحفّاز في مسارات التحلل الضوئي لمُعقدات الروثينيوم (II) متعددة البيريدين.

الكلمات المفتاحية: معقدات الروثينيوم (II) متعددة البيريدين؛ آلية التحلل الضوئي؛ حالات MLCT؛ تنسيق PtI_2 ؛ مطيافية UV-Vis؛ تأثيرات المذيب.

Introduction:

Ruthenium(II) polypyridyl complexes are esteemed as adaptable photosensitizers owing to their robust visible-light absorption, adjustable metal-to-ligand charge-transfer (MLCT) transitions, and remarkable chemical stability. Among the various polypyridyl ligands, 4,4'-di-tert-butyl-2,2'-bipyridine (tbbpy) has attracted particular attention because the sterically demanding tert-butyl substituents enhance solubility in organic media and reduce intermolecular aggregation, while also influencing the electronic environment of the metal center. These structural features can stabilize the MLCT excited state and improve the photochemical robustness of Ru(II) complexes compared with unsubstituted bipyridine analogues. (Fennes et al., 2024)

These attributes have facilitated their widespread use in photochemical and photocatalytic systems. Despite comprehensive research on their coordination environment, comprehending the impact of peripheral ligand modification and solvent interactions on electronic transitions and long-term photostability continues to pose a significant problem (Sun et al., 2010; Lanquist et al., 2023).

The photoexcitation of these complexes promotes MLCT events, in which an electron is elevated from the metal-centered d orbitals to the ligand-based π^* orbitals. The excited state that results demonstrates a lifetime and decay characteristics that are highly dependent on the electronic attributes of the peripheral ligands and the surrounding solvent environment (Suneesh et al., 2014; Di Pietro et al., 2021; Cotic et al., 2024).

Previous studies have shown that the polarity of the solvent and the structure of the ligands play a significant role in modifying spectroscopic and photochemical properties, thus influencing both excited-state dynamics and photostability (Khanduja et al., 2023; Mohammed & Younis, 2025).

This study examines two Ru(II) polypyridyl complexes, each containing tbbpy ligands, which differ by the presence or absence of a ligand-free PtI_2 catalytic unit. Photodegradation kinetics were analyzed under pseudo-first-order conditions using time-dependent UV-Vis absorbance

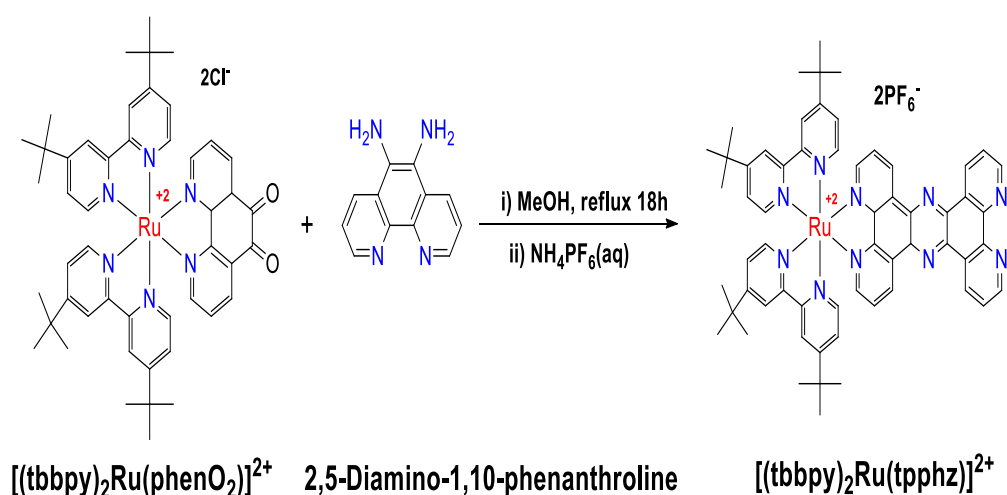
measurements to determine apparent rate constants and half-lives. Complementary HPLC and ^1H NMR analyses were conducted to confirm that changes in absorbance reflected actual chemical degradation by monitoring product formation and structural integrity.

The effect of the PtI_2 catalytic component on photostability was assessed by comparing the two complexes, revealing the influence of the catalytic unit on MLCT lifetime and degradation pathways, independent of catalytic turnover. This integrated approach, which combines kinetic and spectroscopic analyses, offers mechanistic insight into how the presence or absence of a catalytic unit governs the photochemical lifetime of Ru(II) polypyridyl complexes.

2. Experimental

2.1 Materials and Methods

The Ru(II) complexes investigated in this study were prepared following the methodology described by Sven Rau et al. (Scheme 1). The Chem Draw scheme emphasizes the central Ru(bpy) $_2$ core and the differing peripheral ligands. All spectroscopic analyses, including UV–Vis measurements, were conducted on the complexes prepared as described.



Scheme 1. Synthesis of the $[(\text{tbbpy})_2\text{Ru}(\text{tpphz})]^{2+}$ complex via ligand-targeted condensation. (Ruslanova et al., 2002)

2.2 Photochemical Study

Photochemical investigations were carried out at ambient temperature using air-equilibrated solutions in a 1 cm quartz cuvettes. The samples were irradiated with a 10 W blue light-emitting diode (LED) source operating at 470 nm. The emitted light closely matches the solar spectrum in terms of energy distribution. The LED employed in this study was a type A2022-110-BLUE.

2.3 Sample Preparation for Photolysis

Each sample was used as received, without further purification. All photodegradation experiments were conducted under ambient air at room temperature. No measures were taken to remove or control oxygen. Sample solutions were made in the absence of ambient light, wrapped with aluminum foil, and tightly sealed to reduce light exposure and evaporation. Samples were produced immediately before measurements. Complexes were synthesized in acetonitrile and methanol at an approximately concentration of $1 \times 10^{-4}\text{M}$.

To ensure complete dissolution and superior homogeneity of the complexes in various solvents, an ultrasonic bath (Bandelin electronic KG, Germany) was utilized. This process also served

to degas the solutions prior to spectroscopic measurements, ensuring highly accurate and reproducible data with an RSD of less than 3%.

3. Results and Discussion

3.1 ^1H NMR Evidence for Electronic Preorganization of tbbpy

The ^1H NMR spectrum of the peripheral tbbpy ligand, recorded in DMSO-d_6 ($c = 3 \text{ mM}$), displays four diagnostic aromatic proton resonances consistent with the proposed ligand structure (Table 1, Figure 1). The most downfield signal at $\delta 8.48 \text{ ppm}$ (d, $J = 8.2 \text{ Hz}$) is assigned to the N-adjacent H^6 proton, reflecting pronounced deshielding induced by the pyridinic nitrogen. The resonances at $\delta 8.10 \text{ ppm}$ (d, $J = 5.6 \text{ Hz}$) and $\delta 7.85 \text{ ppm}$ (d, $J = 5.6 \text{ Hz}$) correspond to H^5 and H^3 , respectively, with identical coupling constants indicating preserved aromatic symmetry.

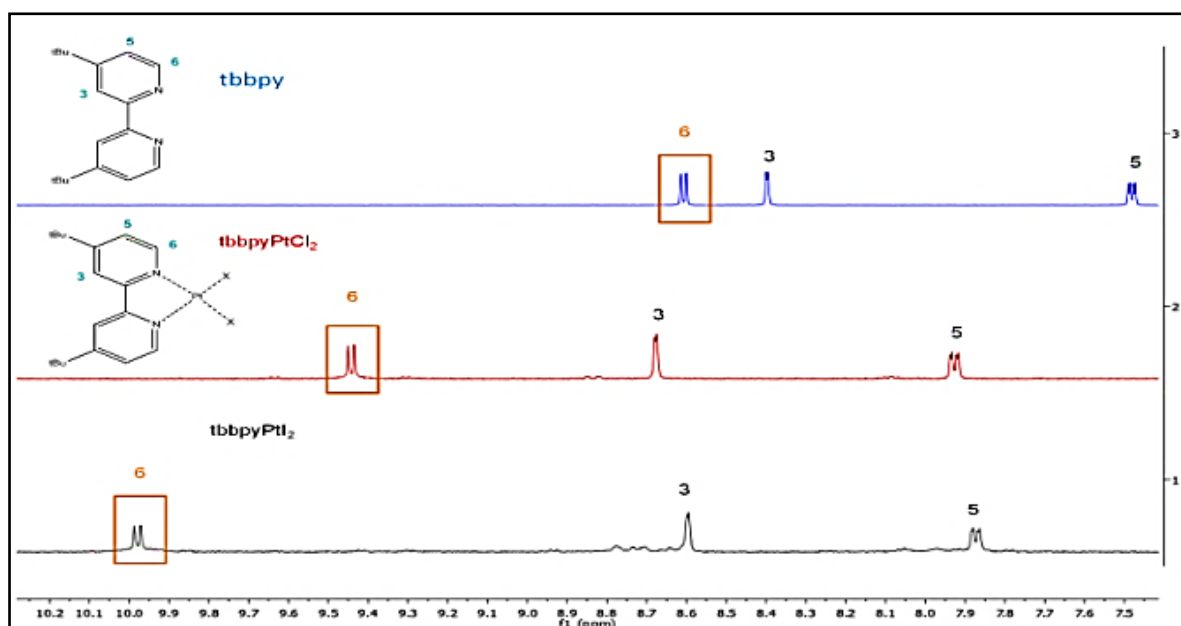


Figure 1: Analysis of the ^1H -NMR spectra of the standard molecule $[\text{Pt}(\text{tbbpy})\text{Cl}_2]$ in DMSO-d_6 . ($c = 3 \text{ mM}$; red: $\text{X} = \text{Cl}$, black: $\text{X} = \text{I}$)

The remaining proton, H^4 , appears as a partially overlapped multiplet in the range $\delta 7.90\text{--}8.20 \text{ ppm}$, attributed to signal congestion within the extended conjugated framework.

Table 1. Diagnostic ^1H NMR protons of the peripheral tbbpy ligand

Proton	δ (ppm)	Multiplicity	J (Hz)	Integration	Relevance to peripheral ligand
H^3	7.85	d	5.6	1H	Aromatic proton sensitive to electronic distribution
H^5	8.10	d	5.6	1H	Symmetry-related aromatic proton
H^6	8.48	d	8.2	1H	N-adjacent proton, strongest deshielding
H^4	7.9–8.2	m	n.r	1H	Partially overlapped, ligand backbone

Notes: Only peripheral ligand protons directly involved in electronic modulation are reported. (*n.r* = not resolved due to overlap).

Collectively, these spectral features confirm the electronic preorganization of the tbbpy ligand, which governs subsequent metal–ligand interactions and enables catalyst-controlled photodegradation in the Ru(II) system.

3.2 HPLC Purity and Chromatographic Stability Analysis

Quantitative evaluation of the HPLC chromatograms (Figure 2) indicates that the synthesized Ru(II) complex exhibits a high level of purity, with an estimated value of approximately 95% based on peak area normalization.

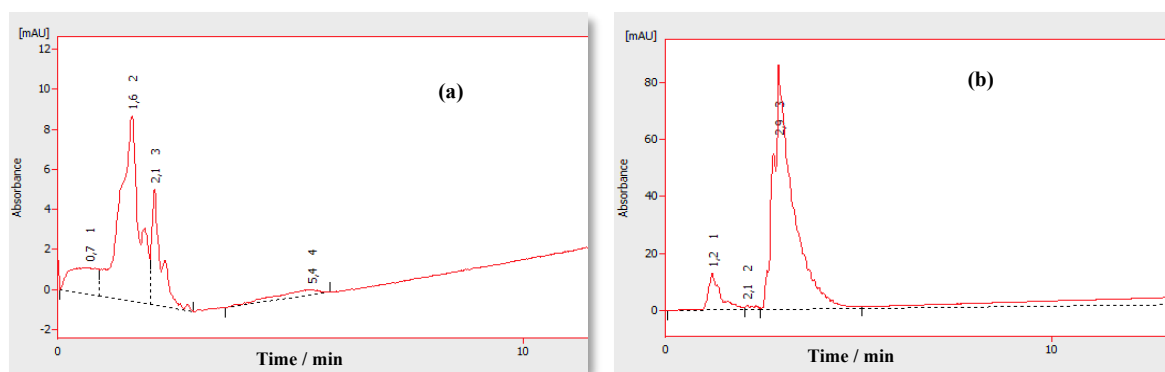


Figure 2: HPLC Signal trace for $[(tbbpy)_2Ru(tpphz)(PtI_2)_2]$ 1×10^{-4} M in (a) CH_3OH , (b) CH_3CN . Mobile phase $CH_3CN: H_2O$ with volume ratio 75: 25 containing 0.1M KNO_3 , Flow rate $2.0 \text{ cm}^3 \text{ min}^{-1}$ -detection wavelength at 254 nm, $T = 24^\circ C$.

The capacity factor (k'), calculated from the retention time of the main chromatographic peak, showed no significant variation upon changing the mobile phase composition and flow rate, indicating stable interaction of the complex with the stationary phase and the absence of detectable decomposition during analysis. Furthermore, SEC/GPC chromatograms (Figure 3) exhibited slight peak broadening, which is attributed to the hydrodynamic behavior of the complex in solution rather than chemical degradation. Collectively, these results confirm the high purity and chromatographic stability of the Ru(II) complex, providing a reliable foundation for subsequent spectroscopic characterization and photochemical investigations.

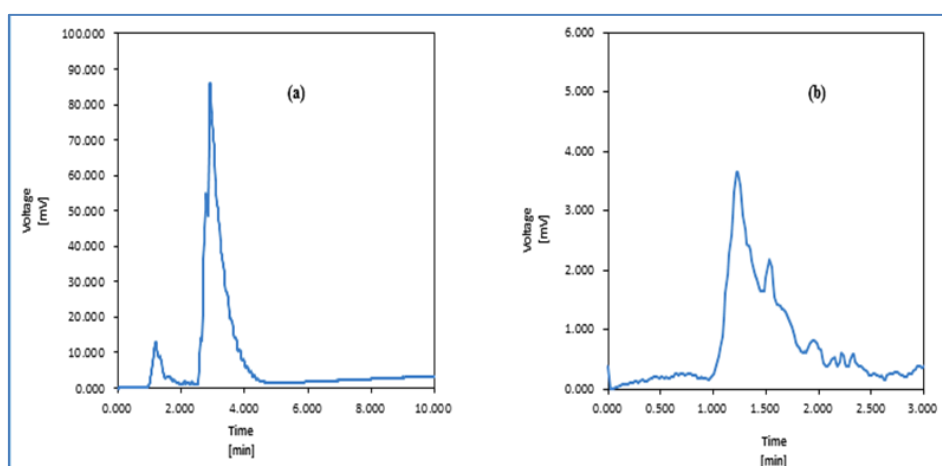


Figure 3: Chromatograms of $[(tbbpy)_2Ru(tpphz)(PtI_2)_2]$ in CH_3OH ; SEC/GPC Columns ($7.8 \times 300 \text{ mm} - 50 \text{ \AA}$); mobile phase, acetonitrile/water (75/25; v/v) and 0.1 M KNO_3 constant; (a) flow rate 2.0 mL/min, (b) flow rate 1.0 mL/min; detection 254 nm.

3.3 UV–Vis and TD-DFT Analysis

The UV–Vis absorption spectra of Ru–tbbpy exhibit a characteristic MLCT band at 446 nm in both acetonitrile and methanol, corresponding to an optical gap of 2.78 eV and an excited-state lifetime in the range of 500–700 ns. A quantitative comparison of the experimental and TD-DFT-derived optical gaps and estimated excited-state lifetimes for Ru–tbbpy and Ru–tbbpy–PtI₂ is presented in Table 2, while the corresponding changes in the MLCT energy levels are schematically illustrated in Figure 4.

Table 2. Optical Gaps (ΔE) and Estimated Excited-State Lifetimes (τ) of Ru–tbbpy Complexes Before and After PtI₂ Coordination.

Complex	Method	Solvent	λ (nm)	ΔE (eV)	τ (ns)	Transition assignment	Trend
Ru–tbbpy	UV–Vis	CH ₃ CN	446	2.78	~500–700	MLCT (Ru($d\pi$) \rightarrow bpy(π^*))	baseline
Ru–tbbpy	UV–Vis	CH ₃ OH	446	2.78	~500–700	MLCT (Ru($d\pi$) \rightarrow bpy(π^*))	baseline
Ru–tbbpy–PtI ₂	TD-DFT (S1)	CH ₃ CN	573.51	2.162	~700–1000	MLCT (Ru($d\pi$) \rightarrow π^* (tpphz))	$\tau \uparrow$, $\Delta E \downarrow$
Ru–tbbpy–PtI ₂	TD-DFT (S1)	CH ₃ OH	572.86	2.164	~700–1000	MLCT (Ru($d\pi$) \rightarrow π^* (tpphz))	$\tau \uparrow$, $\Delta E \downarrow$

As shown, coordination of PtI₂ results in a pronounced red shift of the lowest-energy MLCT transition ($\Delta E \approx 2.16$ eV) and an increase in the estimated τ to ~700–1000 ns. This reflects a stabilization of the acceptor orbitals in the tpphz/Pt fragment and enhanced charge-transfer character, consistent with the energy gap law and previous studies on Ru–polypyridyl systems (Milenković & Zarić, 2020; Wei et al., 2020; García-Camacho et al., 2021). The presence of the heavy Pt atom also promotes intersystem crossing, illustrating a balance between decreased non-radiative decay and increased spin–orbit coupling. Overall, these results demonstrate that PtI₂ coordination significantly modulates both the energetics and dynamics of the MLCT state, highlighting the Ru–Pt assembly as a promising system for photo functional applications.

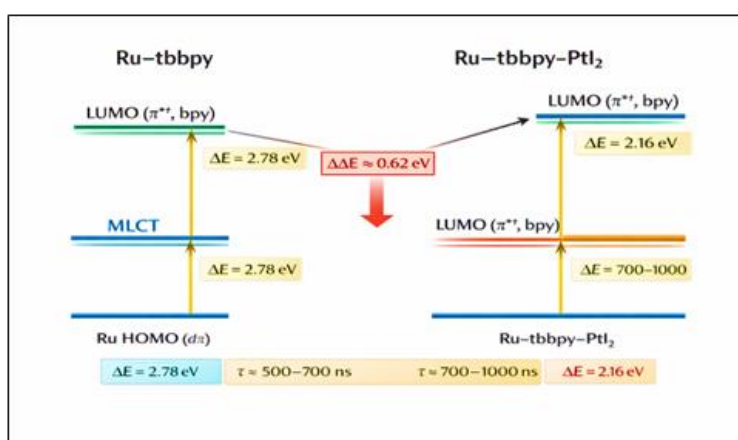


Figure 4. Simplified energy level diagram of Ru–tbbpy and Ru–tbbpy–PtI₂ illustrating the MLCT transitions, optical gaps (ΔE), and estimated excited-state lifetimes (τ).

The apparent formation constant (K_f) for PtI_2 coordination to the Ru–tbbpy complex, as summarized in Table 3, was estimated from changes in the UV–Vis absorption spectra using a Benesi–Hildebrand-type analysis. In this treatment, a 1:1 interaction between Ru–tbbpy and PtI_2 was assumed in order to approximate the initial coordination equilibrium in solution. It should be noted that this spectroscopic approach provides an apparent formation constant corresponding to the first coordination step. Although the final Ru–Pt assembly contains two PtI_2 units in its fully coordinated form, the UV–Vis titration primarily probes the initial interaction between the Ru–tbbpy complex and a single PtI_2 unit. The analysis was carried out at the MLCT absorption band (≈ 484 – 487 nm), which exhibited the most pronounced spectral response upon addition of PtI_2 .

A clear solvent dependence was observed, with a significantly higher apparent formation constant in methanol ($\approx 10^4$ M^{-1}) compared to acetonitrile ($\approx 10^3$ M^{-1}), indicating enhanced thermodynamic stability of the coordination interaction in the protic solvent. This behavior can be attributed to reduced solvent competition and stronger stabilization of the coordination interaction in methanol. In addition to the equilibrium analysis, kinetic parameters were estimated from the time-dependent absorption changes assuming first-order behavior. The resulting rate constants were 0.259 h^{-1} in methanol and 0.296 h^{-1} in acetonitrile, corresponding to half-lives ($t_{1/2}$) of 2.68 h and 2.34 h, respectively. The longer half-life observed in methanol suggests greater kinetic stability of the coordination interaction in this solvent, whereas the slightly shorter half-life in acetonitrile reflects partial competition by the coordinating solvent molecules.

These kinetic trends are consistent with the apparent formation constants and with the TD-DFT calculations, which indicate stabilization of the MLCT excited state upon PtI_2 coordination. Overall, the combined spectroscopic and computational results demonstrate that both the catalytic metal center and the solvent environment play an important role in modulating the thermodynamic and kinetic stability of the Ru–Pt assembly, highlighting its potential relevance for photo-functional applications.

Table 3. Apparent formation constants (K_f), rate constants (k), and half-lives ($t_{1/2}$) for PtI_2 coordination to the Ru–tbbpy complex in different solvents.

Solvent	$K_f(M^{-1})$	$K(h^{-1})$	$t_{1/2}$
CH_3OH	1.0×10^4	0.259	2.68
CH_3CN	1.0×10^3	0.296	2.34

4. Conclusions

The photodegradation behavior of Ru(II) polypyridyl complexes was systematically investigated under visible-light irradiation, providing mechanistic insight into the factors governing their photochemical stability. The results demonstrate that the degradation process follows pseudo-first-order kinetics in both acetonitrile and methanol. Incorporation of a peripheral PtI_2 unit significantly modulates the metal-to-ligand charge-transfer (MLCT) excited state by reducing the optical energy gap and prolonging the excited-state lifetime, which in turn suppresses photodegradation pathways. Complementary UV–Vis, HPLC, and 1H NMR analyses confirm that the observed spectral changes originate from irreversible chemical degradation rather than transient photophysical processes. Solvent-dependent behavior further reveals that methanol enhances both kinetic and thermodynamic stability relative to acetonitrile. Overall, these findings highlight the important role of metal coordination and

solvent environment in controlling the photochemical stability of Ru(II) polypyridyl systems, providing useful insights for the design of more robust photoactive complexes.

5. Acknowledgements

The authors gratefully acknowledge the financial and technical support provided by the Sven Rau Research Group, Germany, which made this research possible. The authors also thank the Chemistry Department, Faculty of Science, Sirte University, for providing laboratory facilities and assistance throughout the study.

6. Conflict of interest: The authors declare that there are no conflicts of interest

7. References

- Cotic, A., Ramírez-Wierzebecki, I., & Cadranel, A. (2024). Harnessing high-energy MLCT excited states for artificial photosynthesis. *Coordination Chemistry Reviews*, 514, 215878. <https://doi.org/10.1016/j.ccr.2024.215878>
- Di Pietro, M. L., La Ganga, G., Nastasi, F., & Puntoriero, F. (2021). Ru(II)-Dppz Derivatives and Their Interactions with DNA: Thirty Years and Counting. *Applied Sciences*, 11(7), 3038. <https://doi.org/10.3390/app11073038>
- Fennes, A., Montesdeoca, N., Papadopoulos, Z., & Karges, J. (2024). Rational design of a red-light absorbing ruthenium polypyridine complex as a photosensitizer for photodynamic therapy. *Chemical Communications*, 60, 10724–10727. <https://doi.org/10.1039/D4CC04126G>
- García-Camacho, F., Martín-Diana, A. B., Nicasio, M. C., & López-García, M. (2021). Excited-state lifetime tuning in transition metal complexes: From fundamentals to applications. *Chemical Society Reviews*, 50(15), 8452–8487. <https://doi.org/10.1039/D1CS00233A>
- Khanduja, D., Singh, A., Sharma, P., Gupta, R., Verma, S., & Kumar, V. (2023). Enhanced photostability and photoactivity of ruthenium polypyridyl-based photocatalysts by covalently anchoring onto reduced graphene oxide. *ACS Omega*, 8(15), 13821–13833. <https://doi.org/10.1021/acsomega.3c08800>
- Lanquist, A. P., Piechota, E. J., Wickramasinghe, L. D., Marques Silva, A., Thummel, R. P., & Turro, C. (2023). New Tridentate Ligand Affords a Long-Lived 3MLCT Excited State in a Ru(II) Complex: DNA Photocleavage and 1O₂ Production. *Inorganic Chemistry*, 62(39), 15927–15935. <https://doi.org/10.1021/acs.inorgchem.3c01990>
- Milenković, D. P., & Zarić, S. (2020). Stacking interactions between indenyl ligands of transition metal complexes: Crystallographic and density functional study. *Crystal Growth & Design*, 20(7), 4491–4502. <https://doi.org/10.1021/acs.cgd.0c00303>
- Mohammed, H. A., & Younis, H. A. (2025, November 30). *Investigation of solvent effects on the spectroscopic and photochemical properties of ruthenium(II) polypyridyl complexes* [Paper presentation]. *Proceedings of the Environmental Pollution and Challenges of Environmental Sustainability Conference (EPESC)*. Sirte University Institutional Repository. <http://dspace-su.server.ly:8080/xmlui/handle/123456789/3595>
- Ruslanova J, Decurtins S, Rusanov E, Stoeckli-Evans H, Delahaye S, Hauser A. Ruthenium(II) complex of bis(2,2'-bipyridine)(6,7-dicyanodipyrido[3,2-a:2',3'-c]phenazine): synthesis,

structure, electrochemical and luminescence studies. *J Chem Soc Dalton Trans.* 2002;(23):4318–4320. <https://doi.org/10.1039/B210440G>

Sun, Y., El Ojaimi, M., Hammitt, R., Thummel, R. P., & Turro, C. (2010). Effect of ligands with extended π -system on the photophysical properties of Ru(II) complexes. *The journal of physical chemistry. B*, 114(45), 14664–14670.

<https://doi.org/10.1021/jp102613n>

Suneesh, C. V., Balan, B., Ozawa, H., Nakamura, Y., Katayama, T., Muramatsu, M., Nagasawa, Y., Miyasaka, H., & Sakai, K. (2014). Mechanistic studies of photoinduced intramolecular and intermolecular electron transfer processes in RuPt-centred photo-hydrogen-evolving molecular devices. *Physical Chemistry Chemical Physics*, 16(4), 1607–1616.

<https://doi.org/10.1039/c3cp54630f>

Wei, H., Li, R., & Zhang, X. (2020). Recent advances in ruthenium(II) polypyridyl complexes: Photophysics, photochemistry and applications. *Coordination Chemistry Reviews*, 416, 213338.

<https://doi.org/10.1016/j.ccr.2020.213338>

Compliance with ethical standards

Disclosure of conflict of interest

The authors declare that they have no conflict of interest.

Disclaimer/Publisher's Note: The statements, opinions, and data contained in all publications are solely those of the individual author(s) and contributor(s) and not of **JLABW** and/or the editor(s). **JLABW** and/or the editor(s) disclaim responsibility for any injury to people or property resulting from any ideas, methods, instructions, or products referred to in the content.